

Evidence of a Pionic Enhancement Observed in

$^{16}\text{O}(p, p')^{16}\text{O}(0^-, T = 1)$ at 295 MeV

T. Wakasa,¹ G. P. A. Berg,² H. Fujimura,³ K. Fujita,⁴ K. Hatanaka,⁴
M. Ichimura,⁵ M. Itoh,⁴ J. Kamiya,⁶ T. Kawabata,⁷ Y. Kitamura,⁴
E. Obayashi,⁴ H. Sakaguchi,³ N. Sakamoto,⁴ Y. Sakemi,⁴ Y. Shimizu,⁴
H. Takeda,⁸ M. Uchida,⁹ Y. Yasuda,³ H. P. Yoshida,¹⁰ and M. Yosoi³

¹*Department of Physics, Kyushu University, Fukuoka 812-8581, Japan*

²*Kernfysisch Versneller Instituut, Zernikelaan 25,
9747 AA Groningen, The Netherlands*

³*Department of Physics, Kyoto University, Kyoto 606-8502, Japan*

⁴*Research Center for Nuclear Physics,
Osaka University, Osaka 567-0047, Japan*

⁵*Faculty of Computer and Information Sciences,
Hosei University, Tokyo 184-8584, Japan*

⁶*Accelerator Group, Japan Atomic Energy Research Institute, Ibaraki 319-1195, Japan*

⁷*Center for Nuclear Study, The University of Tokyo, Tokyo 113-0033, Japan*

⁸*The Institute of Physical and Chemical Research, Saitama 351-0198, Japan*

⁹*Department of Physics, Tokyo Institute of Technology, Tokyo 152-8550, Japan*

¹⁰*Research and Development Center for Higher Education,
Kyushu University, Fukuoka 810-8560, Japan*

(Dated: November 10, 2018)

Abstract

The cross section of the $^{16}\text{O}(p, p')^{16}\text{O}(0^-, T = 1)$ scattering was measured at a bombarding energy of 295 MeV in the momentum transfer range of $1.0 \text{ fm}^{-1} \leq q_{\text{c.m.}} \leq 2.1 \text{ fm}^{-1}$. The isovector 0^- state at $E_x = 12.8$ MeV is clearly separated from its neighboring states owing to the high energy resolution of about 30 keV. The cross section data were compared with distorted wave impulse approximation (DWIA) calculations employing shell-model wave functions. The observed cross sections around $q_{\text{c.m.}} \simeq 1.7 \text{ fm}^{-1}$ are significantly larger than predicted by these calculations, suggesting pionic enhancement as a precursor of pion condensation in nuclei. The data are successfully reproduced by DWIA calculations using random phase approximation response functions including the Δ isobar that predict pionic enhancement.

PACS numbers: 21.60.Jz, 25.40.Ep, 27.20.+n

The search for pionic enhancements in nuclei has a long and interesting history. These phenomena can be considered as a precursor of the pion condensation [1] that would be realized in neutron stars. Enhancements of the $M1$ cross section in proton inelastic scattering [2, 3, 4, 5] and of the ratio R_L/R_T , the spin-longitudinal (pionic) response function R_L to the spin-transverse one R_T , in the quasielastic scattering (QES) region [6, 7] were expected around a momentum transfer $q_{c.m.} \simeq 1.7 \text{ fm}^{-1}$. However, the experimental data did not reveal any pionic enhancements [8, 9, 10]. Several explanations exist to answer the question why no pionic enhancements were observed. For example, Bertsch, Frankfurt, and Strikman [11] suggest the modification of gluon properties in the nucleus that suppresses the pion field. Brown *et al.* [12] suggest the partial restoration of chiral invariance with density. However, we should note that the $M1$ cross section includes both pionic and non-pionic contributions and R_L/R_T is the ratio to the non-pionic R_T . Thus, in these indirect measurements, the pionic enhancement might be masked by the contribution from the non-pionic component. Recent analyses of the QES data [13, 14] show a pionic enhancement in the spin-longitudinal cross section that well represents the R_L , and suggest that the lack of enhancements of R_L/R_T is due to the non-pionic component.

In order to measure the pionic enhancement directly, it is desirable to investigate isovector $J^\pi = 0^-, 0^\pm \rightarrow 0^\mp$ excitations because they carry the same quantum numbers as the pion and they are free from non-pionic contributions. Orihara *et al.* [15] measured the angular distribution of the $^{16}\text{O}(p, n)^{16}\text{N}(0^-, 0.12 \text{ MeV})$ reaction at $T_p = 35 \text{ MeV}$. They reported discrepancies between distorted wave Born approximation calculations and their data in the range of $q_{c.m.} = 1.4\text{--}2.0 \text{ fm}^{-1}$ that might be a signature of pionic enhancement. However, in the proton inelastic scattering to the $0^-, T = 1$ state in ^{16}O at $T_p = 65 \text{ MeV}$, such an enhancement was not observed [16]. The differences between these (p, n) and (p, p') results might indicate contributions from complicated reaction mechanisms at these low incident energies. To our knowledge, there are no published experimental data for the $0^-, T = 1$ state at intermediate energies of $T_p > 100 \text{ MeV}$ where reaction mechanisms are expected to be simple.

In this Letter, we present the measurement of the cross section for the excitation of the $0^-, T = 1$ state at $E_x = 12.8 \text{ MeV}$ in ^{16}O using inelastic proton scattering at 295 MeV incident energy. The results are compared with distorted wave impulse approximation (DWIA) calculations with shell-model (SM) wave functions. Evidence of a pionic enhancement is clearly

observed from a comparison between experimental and theoretical results. The data are also compared with DWIA calculations employing random phase approximation (RPA) response functions including the Δ isobar in order to assess the pionic enhancement quantitatively.

The measurement was carried out by using the West-South Beam Line (WS-BL) [17] and the Grand Raiden (GR) spectrometer [18] at the Research Center for Nuclear Physics, Osaka University. The WS-BL provides the beam with lateral and angular dispersions of 37.1 m and -20.0 rad, respectively, which satisfy the dispersion matching conditions for GR. The beam bombarded a windowless and self-supporting ice (H_2O) target [19] with a thickness of 14.1 mg/cm². Protons scattered from the target were momentum analyzed by the high-resolution GR spectrometer with a typical resolution of ~ 30 keV FWHM. The beam energy was determined to be 295 ± 1 MeV by using the kinematic energy shift between elastic scattering from ^1H and ^{16}O . The yields of the scattered protons were extracted using the peak-shape fitting program ALLFIT [20].

The elastic scattering data on ^{16}O are shown in Fig. 1. Differential cross sections were normalized to the known $p + p$ cross section [21] by utilizing the data of protons scattered from the hydrogen present in the ice target. The data were analyzed using optical model potentials (OMPs) generated phenomenologically. The solid curve in Fig. 1 is the result using the global OMP optimized for ^{16}O [22]. The band represents the results by using several OMPs parametrized for nuclei from ^{12}C to ^{208}Pb with a smooth mass number dependence [22] that shows the ambiguity of the OMP for ^{16}O . The global OMP for ^{16}O reproduces the experimental data reasonably well. The systematic uncertainty for the cross section normalization is estimated to be less than $\sim 10\%$ from this result. In the following, we will use this OMP in DWIA calculations for inelastic scattering.

Figure 2 shows the excitation energy spectrum of the $^{16}\text{O}(p, p')$ scattering at $q_{\text{c.m.}} = 1.9$ fm⁻¹. The isovector 0^- state at $E_x = 12.8$ MeV is clearly resolved from the neighboring states. The dashed curves represent the fits to the individual peaks while the straight line and solid curve represent the background and the sum of the peak fitting, respectively. Narrow peaks of ^{16}O were described by a standard hyper-Gaussian line shape, and the peaks with intrinsic widths were described as Lorentzian shapes convoluted with a resolution function based on the narrow peaks. The positions and widths were taken from Ref. [23].

Figure 3 shows the measured data points and the calculated curves of the cross sections of the 0^- , $T = 1$ transition in $^{16}\text{O}(p, p')$ as a function of the momentum transfer $q_{\text{c.m.}}$. The

angular distribution was measured in the range of $q_{c.m.} \simeq 1.0 \text{ fm}^{-1}$ to $\simeq 2.1 \text{ fm}^{-1}$ starting near the second maximum at $q_{c.m.} \simeq 0.9 \text{ fm}^{-1}$ and extending beyond the third maximum at $q_{c.m.} \simeq 1.7 \text{ fm}^{-1}$. The error bars of the data points are the fitting uncertainties originating from the statistical uncertainties. The shaded areas represent the systematic uncertainties including the background subtraction.

We performed DWIA calculations by using the computer code DWBA98 [24]. The one-body density matrix elements (OBDME) for the isovector 0^- transition of $^{16}\text{O}(p, p')$ were obtained from Ref. [25]. This SM calculation was performed in the $0s-0p-1s0d-0f1p$ configuration space by using phenomenological effective interactions. In the calculation, the ground state of ^{16}O was described as a mixture of $0\hbar\omega$ (closed-shell) and $2\hbar\omega$ configurations. The single particle radial wave functions were generated by using a Woods-Saxon (WS) potential [26], the depth of which was adjusted to reproduce the separation energies of the $0p_{1/2}$ orbits. The unbound single particle states were assumed to have a very small binding energy of 0.01 MeV to simplify the calculations. The NN t -matrix parametrized by Franey and Love [27] at 325 MeV was used. The DWIA result is shown as the solid curve in Fig. 3. The calculation reproduces the data in the lower- $q_{c.m.}$ region reasonably well, but they significantly underestimate the data in the higher- $q_{c.m.}$ region. Also, the data has a maximum at $q_{c.m.} \simeq 1.7 \text{ fm}^{-1}$, whereas the maximum of the theoretical curve is slightly higher at $q_{c.m.} \simeq 1.8 \text{ fm}^{-1}$.

We investigated the sensitivity of the DWIA calculations to changes of the parameters involved. The dash-dotted curve represents the DWIA calculation with a different t -matrix parametrized at 270 MeV. The result is systematically larger compared to the calculation with the t -matrix at 325 MeV. The dash-dotted curve is, therefore, multiplied by a factor of 0.7. The dashed curve denotes the calculation employing a different OBDME with a pure $0p_{1/2}^{-1}1s_{1/2}$ transition from the $0\hbar\omega$ (closed-shell) ground state. Auerbach and Brown [25] suggest that this isovector strength is quenched and spread by a $2\hbar\omega$ admixture. They obtained a quenching factor of ~ 0.64 . Thus we have applied this factor as a normalization factor to the result. We also performed a DWIA calculation with the radial wave functions generated with a harmonic oscillator potential with a size parameter of $\alpha = 0.588 \text{ fm}^{-1}$ [28]. The result is systematically larger compared to the calculation with the WS potential. However, their shapes of the angular distribution are very similar to each other. From these calculations we found that the shape of the angular distribution is insensitive to changes of

the input parameters. Thus it is difficult to understand the discrepancies between experimental and theoretical results within the framework of the standard DWIA employing SM wave functions. Therefore, in the following, we investigate non-locality, RPA correlation, and Δ effects that are not taken into account in these standard calculations.

The non-locality of the nuclear mean field can be included by introducing a local effective mass approximation in the form of

$$m^*(r) = m_N - \frac{f_{\text{WS}}(r)}{f_{\text{WS}}(0)}(m_N - m^*(0)), \quad (1)$$

where m_N is the nucleon mass and $f_{\text{WS}}(r)$ is a WS radial form. The upper panel of Fig. 4 shows the m^* dependence of the DWIA calculations with the free response function that were performed using the computer code CRDW developed by the Ichimura group [29] for the analysis of QES data. The 0^- component of the free response is configured as a pure $0p_{1/2}^{-1}1s_{1/2}$ transition. The DWIA result with $m^*(0) = m_N$ is in good agreement with the calculation employing the corresponding SM wave function represented by the dashed curve in Fig. 3. Thus we have applied the same normalization factor of 0.64 to the results shown in Fig. 4. The angular distribution shifts to lower $q_{\text{c.m.}}$ when decreasing $m^*(0)$. As seen in the upper panel of Fig. 4, a value of $m^*(0)/m_N \simeq 0.7$ improves the agreement with the data, consistent with theoretical estimations [30, 31]. However there is still a large discrepancy between experimental and theoretical results around $q_{\text{c.m.}} \simeq 1.7 \text{ fm}^{-1}$.

Next, we discuss the RPA correlation and Δ effects. We performed DWIA calculations with the RPA response functions employing the $\pi + \rho + g'$ model interaction V_{eff} and the meson parameters from a Bonn potential which treats the Δ explicitly [32]. The V_{eff} is the sum of the one- π and one- ρ exchange interactions, and the Landau-Migdal (LM) interaction V_{LM} specified by the LM parameters, g'_{NN} , $g'_{N\Delta}$, and $g'_{\Delta\Delta}$, as

$$\begin{aligned} V_{\text{LM}} = & \left[\frac{f_{\pi NN}^2}{m_\pi^2} g'_{NN} (\boldsymbol{\tau}_1 \cdot \boldsymbol{\tau}_2) (\boldsymbol{\sigma}_1 \cdot \boldsymbol{\sigma}_2) \right. \\ & + \frac{f_{\pi NN} f_{\pi N\Delta}}{m_\pi^2} g'_{N\Delta} \{ ((\boldsymbol{\tau}_1 \cdot \mathbf{T}_2) (\boldsymbol{\sigma}_1 \cdot \mathbf{S}_2) + \text{h.c.}) + (1 \leftrightarrow 2) \} \\ & \left. + \frac{f_{\pi N\Delta}^2}{m_\pi^2} g'_{\Delta\Delta} \{ (\mathbf{T}_1 \cdot \mathbf{T}_2^\dagger) (\mathbf{S}_1 \cdot \mathbf{S}_2^\dagger) + (1 \leftrightarrow 2) \} \right] \delta(\mathbf{r}_1 - \mathbf{r}_2), \end{aligned} \quad (2)$$

where $\boldsymbol{\sigma}$ ($\boldsymbol{\tau}$) is the nucleon Pauli spin (isospin) matrix, \mathbf{S} (\mathbf{T}) is the spin (isospin) transition operator that excites N to Δ , $f_{\pi NN}$ ($f_{\pi N\Delta}$) is the πNN ($\pi N\Delta$) coupling constant, and m_π is the pion mass. The middle panel of Fig. 4 shows the g'_{NN} dependence for $g'_{NN} = 0.5\text{--}0.8$

in 0.1 steps with the fixed $g'_{N\Delta} = 0.4$ and $m^*(0)/m_N = 0.7$. The lower panel shows the $g'_{N\Delta}$ dependence for $g'_{N\Delta} = 0.2\text{--}0.5$ in 0.1 steps with the fixed $g'_{NN} = 0.7$ and $m^*(0)/m_N = 0.7$. We fixed $g'_{\Delta\Delta} = 0.5$ [33] since the dependence of the calculated results on this parameter is very weak. The calculated angular distributions depend strongly on g'_{NN} in the whole $q_{\text{c.m.}}$ range, whereas a strong $g'_{N\Delta}$ dependence is observed only around $q_{\text{c.m.}} \simeq 1.7 \text{ fm}^{-1}$. The most probable choices are $g'_{NN} \simeq 0.7$ and $g'_{N\Delta} = 0.3\text{--}0.4$. As a result, the V_{eff} in the NN channel are close to zero whereas that in the $N\Delta$ channel becomes very attractive [13]. This attraction causes the pionic enhancement.

In conclusion, our high-resolution measurement of $^{16}\text{O}(p, p')^{16}\text{O}(0^-, T = 1)$ has enabled us to search for a pionic enhancement at an intermediate energy of $T_p = 295 \text{ MeV}$ where the theoretical DWIA calculations are reliable owing to the simple reaction mechanism. A significant enhancement has been observed around $q_{\text{c.m.}} \simeq 1.7 \text{ fm}^{-1}$ compared to standard DWIA calculations with SM wave functions. The DWIA analyses employing RPA response functions with the Δ isobar allowed the determination of $m^*(0)/m_N \simeq 0.7$ and a set of the Landau-Migdal parameters of $g'_{NN} \simeq 0.7$ and $g'_{N\Delta} = 0.3\text{--}0.4$, in good agreement with estimates based on other experimental data [14]. The present direct measurement strongly indicates the existence of the pionic enhancement in nuclei that may be attributed to a precursor phenomena of the pion condensation.

We thank the RCNP cyclotron crew for providing a good quality beam. This work was supported in part by the Grants-in-Aid for Scientific Research Nos. 12740151, and 14702005 of the Ministry of Education, Culture, Sports, Science, and Technology of Japan.

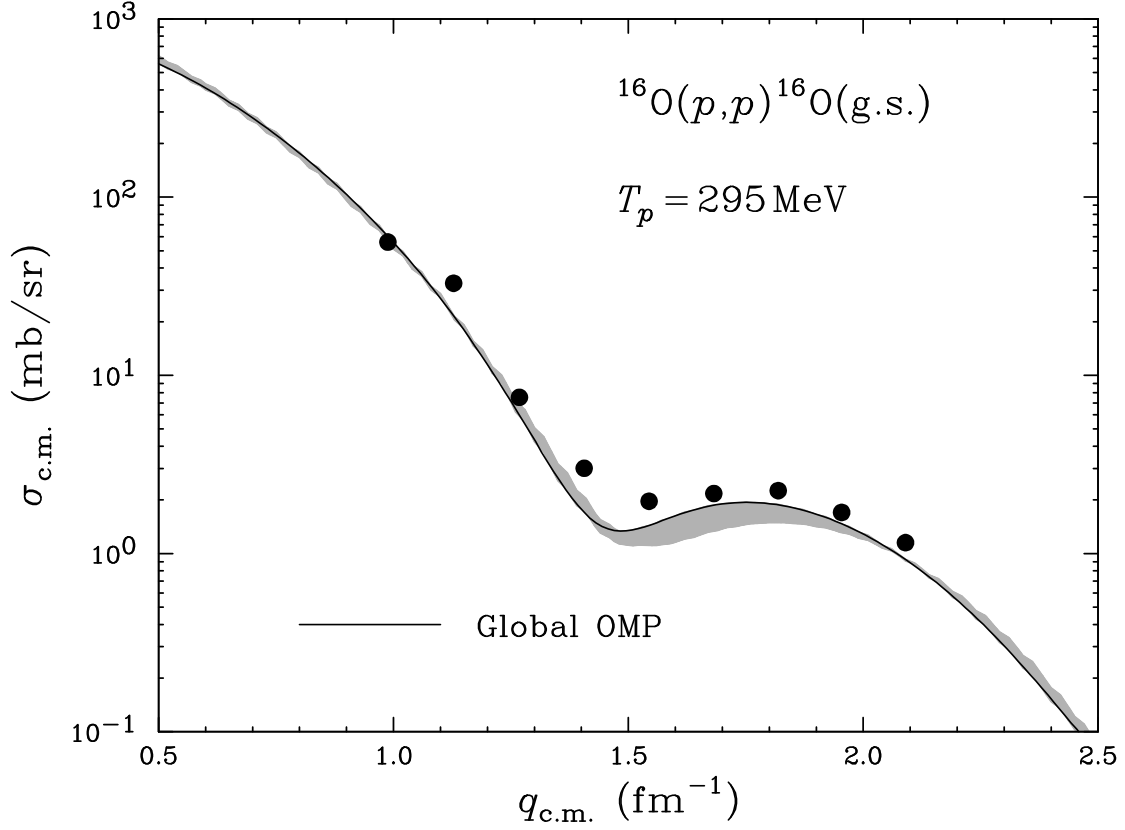


FIG. 1: The measurement of the cross section for $^{16}\text{O}(p,p)$ at $T_p = 295 \text{ MeV}$. The solid curve is the theoretical prediction using the global OMP for ^{16}O . The band represents the ambiguity of the prediction as explained in the text.

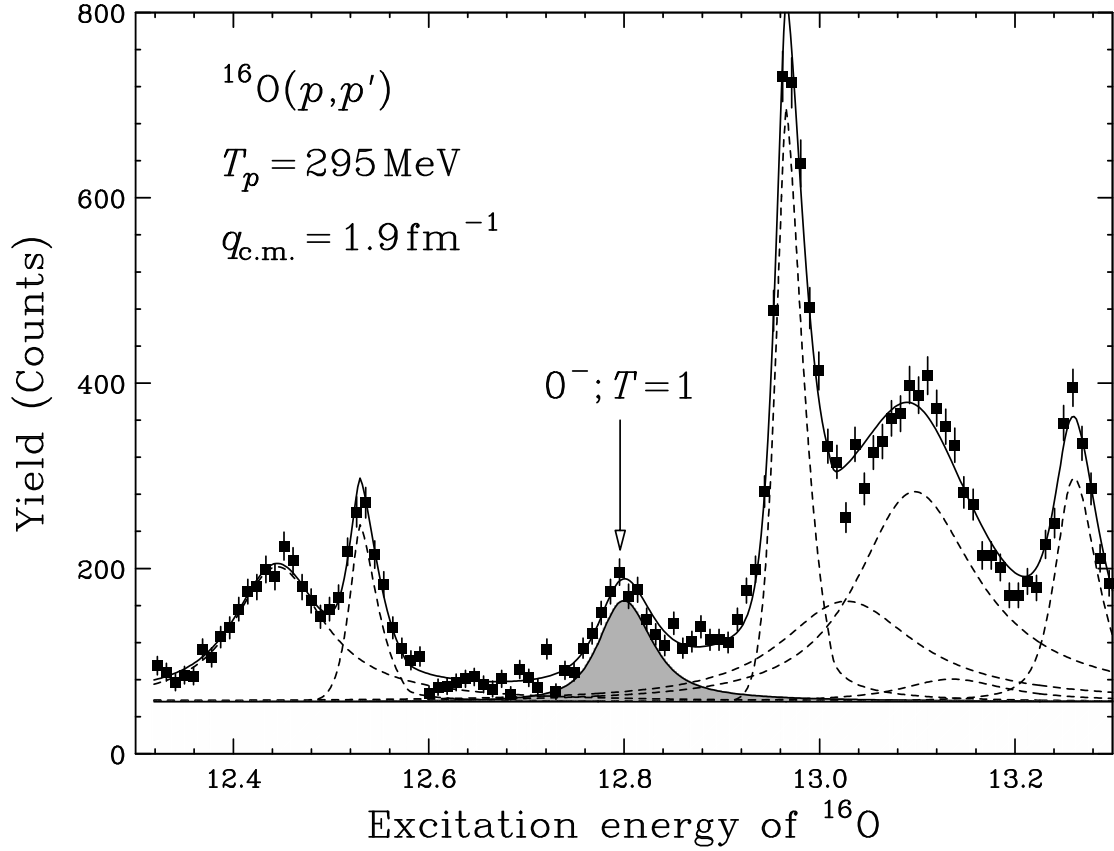


FIG. 2: The excitation energy spectrum for $^{16}\text{O}(p, p')$ at $T_p = 295 \text{ MeV}$ and $q_{\text{c.m.}} = 1.9 \text{ fm}^{-1}$. The curves show the reproduction of this spectrum with hyper-Gaussian and Lorentzian peaks and a continuum.

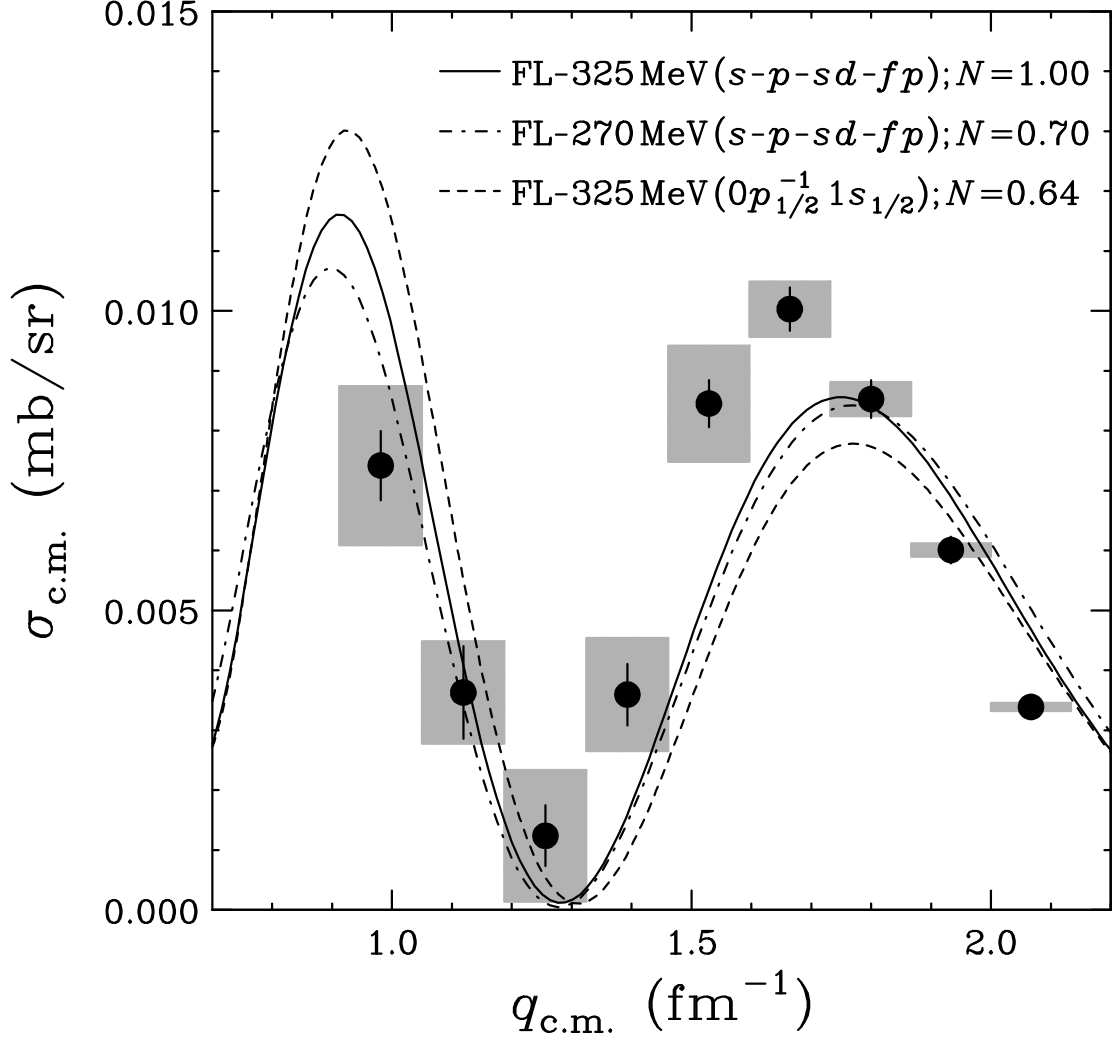


FIG. 3: The measurement of the cross section of $^{16}\text{O}(p, p')^{16}\text{O}(0^-, T = 1)$ at $T_p = 295$ MeV. The shaded areas represent the systematic uncertainties of the data. The solid (dash-dotted) curve is the DWIA result with the t -matrix parametrized at 325 (270) MeV employing the SM wave function in the $0s-0p-1s0d-1p0f$ model space. The dashed curve denotes the DWIA result with the t -matrix at 325 MeV employing the pure $0p_{1/2}^{-1}1s_{1/2}$ SM wave function.

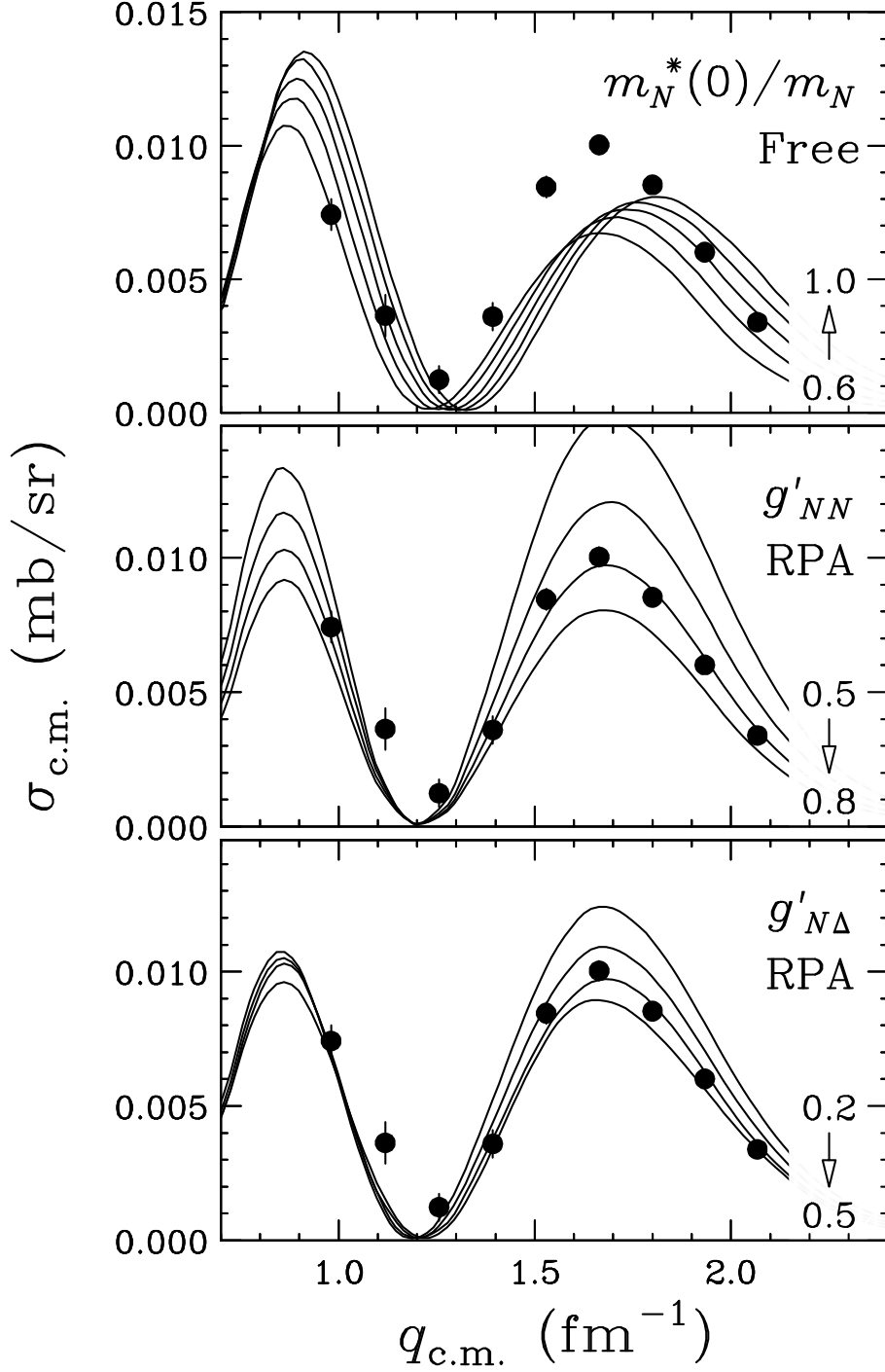


FIG. 4: The top panel shows the $m^*(0)/m_N$ dependence of the DWIA calculations with the free response function. The middle panel represents the g'_{NN} dependence of the calculations employing the RPA response function with fixed $g'_{N\Delta} = 0.4$ and $m^*(0)/m_N = 0.7$. The bottom panel denotes the $g'_{N\Delta}$ dependence of the calculations employing the RPA response function with fixed $g'_{NN} = 0.7$ and $m^*(0)/m_N = 0.7$. The curves in each panel represent calculations where the parameters in the ranges shown are changed in steps of 0.1.

-
- [1] A. B. Migdal, Zh. Eksp. Teor. Fiz. **61**, 2210 (1971); Sov. Phys. JETP **34**, 1184 (1972).
- [2] H. Toki and W. Weise, Phys. Rev. Lett. **42**, 1034 (1979).
- [3] J. Delorme *et al.*, Phys. Lett. **89B**, 327 (1980).
- [4] J. Delorme, A. Figureau, and N. Giraud, Phys. Lett. **91B**, 328 (1980).
- [5] H. Toki and W. Weise, Phys. Lett. **92B**, 265 (1980).
- [6] W. M. Alberico, M. Ericson, and A. Molinari, Phys. Lett. **92B**, 153 (1980).
- [7] W. M. Alberico, M. Ericson, and A. Molinari, Nucl. Phys. **A379**, 429 (1982).
- [8] J. R. Comfort *et al.*, Phys. Rev. C **23**, 1858 (1981).
- [9] T. N. Taddeucci *et al.*, Phys. Rev. Lett. **73**, 3516 (1994).
- [10] T. Wakasa *et al.*, Phys. Rev. C **59**, 3177 (1999).
- [11] G. F. Bertsch, L. Frankfurt, and M. Strikman, Science **259**, 773 (1993).
- [12] G. E. Brown *et al.*, Nucl. Phys. A **593**, 295 (1995).
- [13] T. Wakasa *et al.*, Phys. Rev. C **69**, 054609 (2004).
- [14] T. Wakasa, M. Ichimura, and H. Sakai, nucl-ex/0411055.
- [15] H. Orihara *et al.*, Phys. Rev. Lett. **49**, 1318 (1982).
- [16] K. Hosono *et al.*, Phys. Rev. C **30**, 746 (1984).
- [17] T. Wakasa *et al.*, Nucl. Instrum. Methods Phys. Res. A **482**, 79 (2002).
- [18] M. Fujiwara *et al.*, Nucl. Instrum. Methods Phys. Res. A **422**, 484 (1999).
- [19] T. Kawabata *et al.*, Nucl. Instrum. Methods Phys. Res. A **459**, 171 (2001).
- [20] J. J. Kelly, computer code ALLFIT (<http://www.physics.umd.edu/enp/jkelly/ALLFIT/allfit.html>).
- [21] R. A. Arndt *et al.*, computer code SAID (<http://gwdac.phys.gwu.edu/>).
- [22] S. Hama *et al.*, Phys. Rev. C **41**, 2737 (1990).
- [23] F. Ajzenberg-Selove, Nucl. Phys. **A375**, 1 (1982).
- [24] J. Raynal, computer code DWBA98, NEA 1209/05, 1999.
- [25] N. Auerbach and B. A. Brown, Phys. Rev. C **65**, 024322 (2002).
- [26] A. Bohr and B. R. Mottelson, *Nuclear structure* (Benjamin, New York, 1969).
- [27] M. A. Franey and W. G. Love, Phys. Rev. C **31**, 488 (1985).
- [28] T. Kawabata *et al.*, Phys. Rev. C **65**, 064316 (2002).
- [29] K. Kawahigashi *et al.*, Phys. Rev. C **63**, 044609 (2001).

- [30] N. V. Giai and P. V. Thieu, Phys. Lett. **126B**, 421 (1983).
- [31] C. Mahaux and R. Sartor, Nucl. Phys. **A481**, 381 (1988).
- [32] R. Machleidt, K. Holinde, and C. Elster, Phys. Rep. **149**, 1 (1987).
- [33] W. H. Dickhoff *et al.*, Phys. Rev. C **23**, 1154 (1981).